

# GENERATION AND GROWTH OF CONDENSED PHASE IN HIGH-VELOCITY FLOWS

G. A. SALTANOV, L. I. SELEZNEV and G. V. TSIKLARI

Moscow Power Engineering Institute, Moscow, U.S.S.R.

(Received 2 June 1971)

**Abstract**—Theoretical and experimental results are considered of spontaneous steam condensation in ultrasonic nozzles. Experimental investigations were carried out in the range of initial pressures from  $10^2$  N/m<sup>2</sup> to  $32 \cdot 10^5$  N/m<sup>2</sup> using optical and thermopneumometric methods. The data are obtained on condensation onset, a shape of a zone of intense phase conversions, particle dimensions measured by a Ne-He laser using the indicatrix asymmetry method. Calculations are also carried out. It is shown that introduction of the coefficient  $\beta > 1.0$  which is a correction for nucleation work into the exponent of the nucleation rate yields good agreement between the predicted and experimental values both for pressure distribution and for the particle dimensions. The relation between  $\beta$  and  $P_0$  in the pressure range investigated is obtained by comparing experimental and predicted data.

## NOMENCLATURE

$c$ ,	velocity;
$\rho$ ,	density;
$T$ ,	temperature;
$P$ ,	pressure;
$i$ ,	enthalpy;
$R$ ,	gas constant;
$B$ ,	compressibility;
$\delta$ ,	surface tension coefficient;
$K$ ,	Boltzman constant;
$L$ ,	latent heat of vaporization;
$J$ ,	nucleation rate;
$\alpha$ ,	phase conversion rate;
$F$ ,	cross-sectional area of a channel;
$\lambda$ ,	light wave length;
$\alpha_k$ ,	condensation coefficient;
$C_p, C_v$ ,	heat capacities of steam at $P = \text{const}$ and $V = \text{const}$ , respectively;
$m$ ,	droplet mass;
$m_0$ ,	molecular mass of condensing material;
$V_m$ ,	volume per one molecule in a condensed phase;
$r_*$ ,	critical dimension of nucleus.

## Subscripts

$s$ ,	saturation;
$k$ ,	condensed phase; condensation onset;
$0$ ,	stagnation;
$*$ ,	critical dimension of droplet.

IN RECENT years rapid development of gas dynamics of non-equilibrium supersaturated and two-phase fluids is observed that may be primarily attributed to practically important problems which have arisen both in classic and in new branches of science and technology. The problems concerned with generation, growth of condensed phase and an effect of non-equilibrium inter-phase heat transfer on the behaviour of high-velocity supersaturated and moist vapour flows are important in wind tunnels, turbines when a vapour expansion process begins at the saturation line, in a number of transport units and power-plants, etc.

Now we shall consider the main peculiarities and relationships of supersaturated condensing fluids at high velocities.

## 1. EQUATIONS OF MOTION OF CONDENSING VAPOUR

The theory of supersaturated condensing vapour flow is based on a combination of kinetic concepts of generation and growth of stable condensation nuclei with general relationships for gas dynamics. Oswatitsch was the first who tried to develop such a theory [1]. Further, the theory was attacked by many investigators and, in particular, at the Moscow Power Engineering Institute [2].

Now we shall consider supersaturated flows when the initial state corresponds to a single-phase region (superheated vapour) or saturation. In the analysis the following assumptions are made

1. The flow is one-dimensional and steady.
2. Velocities of the phases are equal.
3. Effects of viscosity and heat conduction of vapour are displayed only when interacting with a condensed phase.
4. Homogeneous spontaneous condensation is assumed, no foreign admixtures (solids, droplets, etc.) at the inlet.
5. Vapour is an ideal gas.

In this case a system of equations for a condensing vapour takes the form

Continuity equation

$$\frac{d\rho cF}{dz} = -\kappa F. \quad (1)$$

Momentum equation

$$\rho c \frac{dc}{dz} + \frac{dp}{dz} = 0. \quad (2)$$

Energy equation

$$\rho c \frac{di_0}{dz} = \kappa(i - \mu_f) + Q. \quad (3)$$

Here  $i = i + c^2/2$  is the complete stagnation enthalpy of the vapour phase;  $\mu_f$  is the thermodynamic potential of the substance undergoing phase conversions; for the case considered  $\mu_f = i - TS$  may be written;  $Q$  is the heat quantity received or released by vapour as a result of

heat transfer between particles of the condensed phase.

A system of equations (1)–(3) may be extended by thermal and caloric equations of state

$$P = \rho R_B T \quad (4)$$

where  $R_B = BR$

$$i = \frac{\gamma}{\gamma - 1} \frac{P}{\rho} + \text{const}, \quad (5)$$

herein  $\gamma = C_p/C_v$ .

An equation for vapour entropy reads

$$S = S_{in} + \frac{R_B}{\gamma - 1} \ln \left[ \frac{P}{P_{in}} \left( \frac{\rho_{in}}{\rho} \right)^\gamma \right] \quad (6)$$

where  $S_{in}$ ,  $P_{in}$ ,  $\rho_{in}$  are the initial entropy, pressure and vapour density, respectively.

The rate of phase conversions  $\kappa$  may be expressed in terms of the nucleation rate and that of phase conversions on the condensed phase particles as follows [3]

$$\kappa = \frac{1}{F} \int_{z_0}^z J(\xi) \frac{dm(\xi, z)}{dz} F(\xi) d\xi + J(z) \cdot m_*(z) \quad (7)$$

where  $m_*(z)$  is the nuclei mass in the cross-section  $z$ .

Up to present several relationships have been obtained for  $J$  giving different values but of the form similar to that of the Frenkel–Zeldovich's formula [4]. A similar equation for  $J$  was used in the present investigation

$$J = \left( \frac{P}{kT} \right)^2 V_m \sqrt{\frac{2\delta}{\pi m_0}} \exp \left[ -\beta \frac{\Delta W(r_*)}{kT} \right]. \quad (8)$$

A nucleation work  $\Delta W(r_*)$  is determined by the formula [5]

$$\Delta W(r_*) = \frac{4}{3} \pi r_*^2 \delta \quad (9)$$

where

$$r_* = \frac{2 \delta V_m}{\Delta \mu}. \quad (10)$$

In reference [5]  $V_m = 1/\rho_k$  is assumed where  $\rho_k$  is the liquid density and  $\Delta \mu$  is the difference of

specific thermodynamic potentials of vapour and condensed phase. It is also assumed that  $\rho_k$ ,  $\delta$  and  $\Delta\mu$  are independent of nuclei dimensions and equal to appropriate values for droplets composed of a great number of molecules. At relatively small subcoolings  $\Delta T = T_s - T$  (where  $T_s$  is the saturation temperature) the potential difference may be determined by the equation [5]

$$\Delta\mu = L \frac{\Delta T}{T}. \quad (11)$$

For correction of the nucleation work  $\Delta W(r_k)$  defined by formula (9) the coefficient  $\beta$  is introduced into the exponential factor of equation (8). It will be shown below that in a general case  $\beta$  is not constant and depends on thermo-physical properties and parameters of the condensing material. With  $\beta = 1$  equation (8) turns into Frenkel-Zeldovich's one.

Now we pass over to a general analysis of the system. Let's start with consideration of an effect of non-equilibrium interphase mass trans- on distribution of gas dynamic parameters with expansion of condensing vapour in a channel of a variable section. With this end in view we write an expression for the derivative  $dP/dz$  in an explicit form that may be easily obtained from equations (1)–(3)

$$\frac{dP}{dz} = \frac{\frac{1}{F} \frac{dF}{dz} - A_x \cdot \kappa - \frac{\gamma - 1}{c} M^2 \cdot Q}{1 - M^2}. \quad (12)$$

Here

$$A_x = c \left[ \frac{\gamma - 1}{a^2} (i - \mu_f) - 1 \right]; a^2 = \gamma \frac{P}{\rho};$$

$$M^2 = c^2/a^2.$$

Using equation (12), we consider the most characteristic types of pressure distribution curves. Predictions show that in the case under consideration an effect of heat transfer  $Q$  on flow parameters is inconsiderable compared to that of the phase conversion rate  $\kappa$ . Therefore,

we restrict here by the analysis of two effects, namely those of the geometry  $dF/dz$  and of phase conversions  $\kappa$ . In a general case the sign of  $A_x$  is indefinite though for steam in a region being far from a critical one  $A_x > 0$ . In a contracting section of the supersonic nozzle  $dF/dz < 0$ , the rate of phase conversions with condensation  $\kappa > 0$ ,  $M < 1$  and hence  $dP/dz < 0$ . In an expanding section of the channel  $dF/dz > 0$ ,  $M > 1$  and a sign of the numerator in this case is determined by an algebraic sum of two terms [ $\omega_F = (1/F)(dF/dz)$ ,  $\omega_x = \kappa(A_x)$ ] with various signs. Curves of static pressure distribution in a zone of spontaneous condensation may be of different shapes depending on the relation between  $\omega_F$  and  $\omega_x$ .

1. The effect of phase conversions in a zone of spontaneous condensation prevails over the geometric effect

$$(\omega_x)_k > (\omega_F)_k.$$

In this case an intense peak of pressure (condensation wave) is observed.

2.  $(\omega_x)_k \approx (\omega_F)_k$ . Pressure peak disappears; a "plateau" in the pressure distribution curve is found in a zone of spontaneous condensation.

3.  $(\omega_x)_k < (\omega_F)_k$ . In spite of intense heat supply the static pressure continues falling and only in the condensation zone the rate of falling decreases.

Vapour temperature in the condensation zone will always grow due to release of phase transition heat.

## 2. EXPERIMENTAL RESULTS AND PHYSICAL ANALYSIS

Conclusions drawn from the analysis of equation (12) are fully confirmed by experimental data. Figure 1 is a plot of static pressure at expansion of condensing vapour in Laval nozzles. Here initial conditions were approximately the same ( $P_0 \approx 1.0 \text{ kg/cm}^2$  and  $T_0 \approx 380^\circ \text{K}$ ), however, an intensity of the geometric effect  $dF/dz$  and therefore expansion velocity  $\dot{P} = -(c/P)(dP/dz)$  considerably differ. (Thus,  $(\dot{P})_1$  differs from  $(\dot{P})_5$  more than by one order,

Table 1

$Z \cdot 10^2 \text{m}$	4.0	4.5	5.0	5.5	6.0	6.5	6.8
$q = F_*/F$	1.000	0.910	0.824	0.735	0.662	0.594	0.562

the point "K" corresponds to the maximum value of the flow subcooling, and the point "B" approximately corresponds to its minimum) First of all it should be noted that as  $\dot{P}$  (and  $dF/dz$ ) increases, the process becomes more non-equilibrium and the zone of spontaneous condensation is shifted down the flow into a

region with larger subcoolings and  $M$  numbers. At the same time three types of  $P$ -distribution curves may be found; the expansion velocity increases with  $dF/dz$ , static pressure curves are transformed exactly following equation (12)\*.

Figure 2 gives pressure distribution curves in a supersonic nozzle for different initial pressures

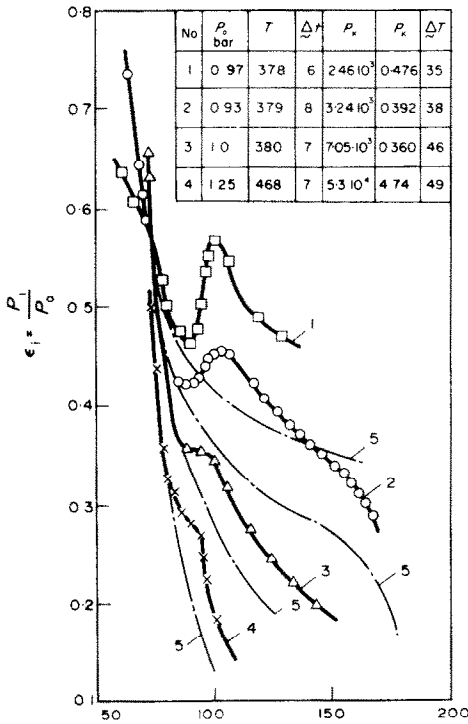


FIG. 1. Static pressure curves in the flow core for vapour expansion in nozzles at various expansion rates. (1)  $P_k = 0.246 \cdot 10^4$  I/s; (2)  $P_k = 0.324 \cdot 10^4$  I/s; (3)  $P_k = 0.705 \cdot 10^4$  I/s; (4)  $P_k = 5.30 \cdot 10^4$  I/s; (5) superheated vapour.

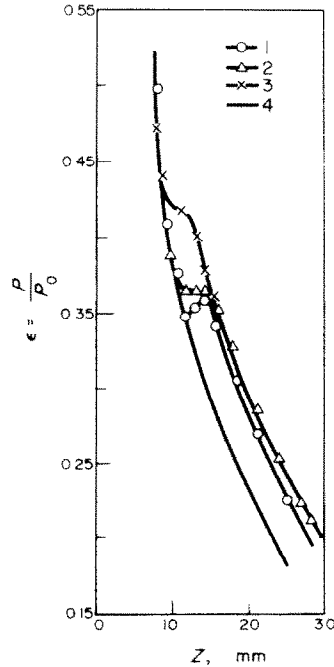


FIG. 2. Pressure distribution in a Laval nozzle at various initial pressures  $P_0$  for  $T_0 - T_{os} = 3^\circ$ . (1)  $P_0 = 6.83$  kg/cm<sup>2</sup>. (2)  $P_0 = 18$  kg/cm<sup>2</sup>; (3)  $P_0 = 25$  kg/cm<sup>2</sup>; (4) superheated vapour.

\* It may be easily shown that in a pure gas flow the expansion velocity  $\dot{P}$  may be expressed in terms of  $dF/dz$  using the law of effect inversions. In this case we have

$$\dot{P} = \frac{kM^2}{M^2 - 1} \frac{c}{F} \frac{dF}{dz}$$

$P_0$ . Parameters of a supersonic section of the nozzle considered are presented in Table 1.

The length of the subsonic section is  $z_2 = 4 \cdot 10^{-2}$  m. The diameter of the nozzle throat is  $d_{cr} = 8.11 \cdot 10^{-3}$  m, an expanding section of the nozzle is a cone with a semiapex angle  $\delta = 3^\circ$ , 26 mm in length. The Mach number at the nozzle section predicted for an ideal gas with  $\gamma = 1.3$  is equal to  $M_p = 2.0$ .

As the initial pressure  $P_0$  increases with vapour expansion from a state close to saturation, the zone of spontaneous condensation displaces up the flow, the pressure peak in this zone flattens. Experiments reveal that in the nozzle considered at  $P_0 < 12 + 13$  kg/cm<sup>2</sup> a supply of condensation heat is accompanied by an adverse pressure gradient ("condensation wave"). At  $P_0 > 13$  kg/cm<sup>2</sup>, other conditions being equal, the proper "condensation wave" is not observed and pressure in a spontaneous condensation zone keeps falling though not so rapidly as in a case of no phase conversions.

Determination of two-phase flow structure appears to be one of the most important and complicated problems in the study of flows with phase conversions.

Under a flow structure both its wave structure (condensation waves, shock waves, rarefaction waves) and a dispersion of a condensed phase and its concentration are understood. In experiments on a condensing vapour structure optical methods were used. A wave structure was investigated using direct-shadow methods. For this purpose flat nozzles with side walls of optical glass were placed in the field of the shadow device IAB-451 [2, 6].

Droplet sizes were found by optical methods of scatter [7] and attenuation [6] of light passing through a two-phase medium. A neon-helium laser was used in the dissipation method as a light source; as for the attenuation method, use was made of a mercury lamp with filters passing-through light of the required wave lengths. Scattered light intensity was measured with the help of photomultipliers.

Now we consider some characteristic results

of experimental study of a steam flow with condensation in a flat supersonic nozzle. Figure 3 gives graphs of static pressure distribution in a nozzle with the calculated Mach number  $M_p = 1.57$  for a flow of superheated (curve 7, initial parameters at a nozzle inlet being  $T_0 = 440^\circ\text{K}$ ,  $P_0 = 0.92 \cdot 10^5$  N/m<sup>2</sup>) and condensing (curve 6,  $P_0 = 0.92 \cdot 10^5$  N/m<sup>2</sup>,  $T_0 = 379^\circ\text{K}$ ) vapour. It

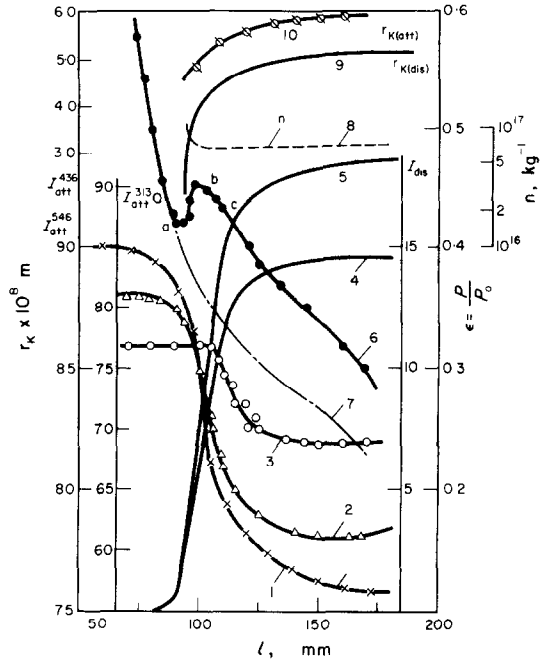


FIG. 3. Determination of dispersion of a condensed phase in a flat Laval nozzle. (1, 2, 3) intensity of weakened light with the wave lengths  $\lambda_1 = 0.313\mu$   $\lambda_2 = 0.436\mu$   $\lambda_3 = 0.546\mu$ ; (4, 5) light scattered intensity in "backward" and "forward" directions; (6, 7) pressure distribution of condensing and superheated vapour; (8) an average number of droplets per mass mixture unit; (9) a mean size of droplets measured by the scattering method; (10) a mean size of droplets measured by the light attenuation method.

may be seen that condensation is accompanied by a noticeable pressure peak (condensation wave). A shadow picture also testifies to a presence of spasmodic change of flow parameters and moreover, it makes possible an exact determination of a spontaneous condensation coordinate.

In Fig. 3 for condensation flows light scatter intensities are plotted measured at  $\gamma_1 = 20^\circ$  and  $\gamma_2 = 160^\circ$  [6, 7]. Experiments show that vapour expansion in a nozzle proceeds with an essential delay of condensation. In practice there are no droplets in a flow up to a critical nozzle section and down the flow that is confirmed by no light dissipation present in the flow. Light scatter on condensation particles begins approximately from point *O* at  $M \simeq 1.3$  and subcooling  $\Delta T \simeq 30^\circ$ . It is worth noting that the point *O* is located up the flow from a zone of the maximum pressure peak and condensation wave (Fig. 3). Then down the flow an intensity of scattered light increases; this increase is especially sharp between sections *a* and *c*. Since the scattered light intensity is proportional to the product  $n \cdot \bar{r}_k^{6*}$ , which implies that in the region between sections *a* and *c* a rapid condensation proceeds that results in increased static pressure and decreased flow velocity in a supersonic nozzle (curve 6, Fig. 3). The flow has achieved a state close to equilibrium one (point *c*), a rate of changing scattered light intensity and therefore a growth of condensed phase particles considerably decrease. Using the indicatrix asymmetry method [7] it is possible to find the mean droplet radius  $\bar{r}_k$  (curve 9) from the ratio  $I_2/I_1$  of the light intensities in the "forward" and "backward" directions (curves 5 and 4).

The same figure furnishes curves of light attenuation passing through a two-phase medium (curves 1, 2, 3). These relations are plotted by experimental data for different wave lengths of passing-through light ( $I, \lambda_1 = 0.313\mu$ ,  $2, \lambda_2 = 0.436\mu$ ,  $\lambda_3 = 0.546\mu$ ). It is seen that the maximum rate of light intensity decrease is found in the spontaneous condensation zone. Using these curves, an average dimension of

\* Here  $n$  is the number of droplets in a lighted volume unit.  $r_k$  is the average radius close to the mean mass radius defined by the formula

$$r_k = \left[ \frac{1}{n} \int_{r_{\min}}^{r_{\max}} f(r) r^6 dr \right]^{1/6}; \quad n = \int_{r_{\min}}^{r_{\max}} f(r) dz;$$

where  $f(r)$  is the size distribution of particles.

droplets (curves 10) as well as condensation of droplets [6] may be determined. It should be noted that this method gives the values of  $r_k$  not so accurate as the scattering method. However, combination of both methods allows simultaneous determination of both size (by scattering) and concentration of particles (by the attenuation method) with a sufficient accuracy.

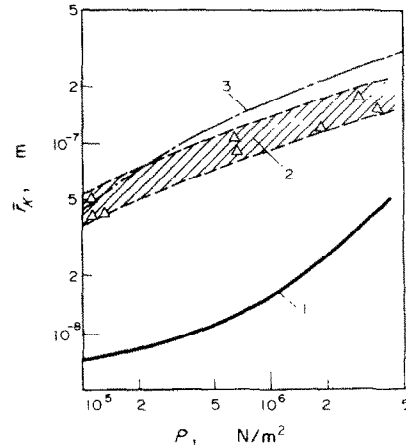


FIG. 4. Mean dimension of droplets at nonequilibrium vapour condensation in a nozzle versus initial pressure  $P_0$  (expansion from the saturation line). (1) prediction following [10] ( $\beta = 1.0$ ); (2) experiment; (3) predicted at  $\beta$ -var.

With an increase of the initial pressure, other conditions being equal, sizes of condensed phase particles increase in the similar sections. In Fig. 4 mean droplet radii are plotted measured at the outlet section by the indicatrix asymmetry method over a wide range of initial pressures  $P_0$ . (Plots of pressure distribution and process parameters for this case are given in Fig. 2.)

It is seen that as  $P_0$  increases from  $10^5$  N/m<sup>2</sup> up to  $32 \cdot 10^5$  N/m<sup>2</sup> the mean droplet radius increases from  $\bar{r}_k = (3-4) \cdot 10^{-8}$  m up to  $\bar{r}_k \simeq 2 \cdot 10^{-7}$  m, i.e. approximately by one order.

Thus, pneumometric as well as optical investigations also present evidence that vapour expansion in confuser channels is an essentially

non-equilibrium process; break-down of supersaturation state proceeds spasmodically on a comparatively short length of the nozzle where a medium comes to a state close to equilibrium.

**3. THEORETICAL PREDICTION AND COMPARISON WITH EXPERIMENT**

The set of equations (1)–(11) was used for an analysis and prediction of a saturated vapour flow in supersonic nozzles investigated experimentally (Section 2). With the assumption that particle dimensions in the case considered are smaller than free molecular path lengths, the steam condensation rate is found by the equation [8]

$$\frac{dm(\xi, z)}{dt} = \frac{\alpha_k 4\pi r_k^2(\xi, z) P}{\sqrt{(2\pi R_B T_n)}} \left( 1 - \frac{P_k}{P} \sqrt{\frac{T}{T_k}} \right). \quad (13)$$

Here  $P_k$  is the saturation pressure in a droplet,  $T_k$  is the droplet temperature which was considered uniform in the droplet volume and equal to saturation temperature  $T_s$  (in this case  $P_k = P$ ).

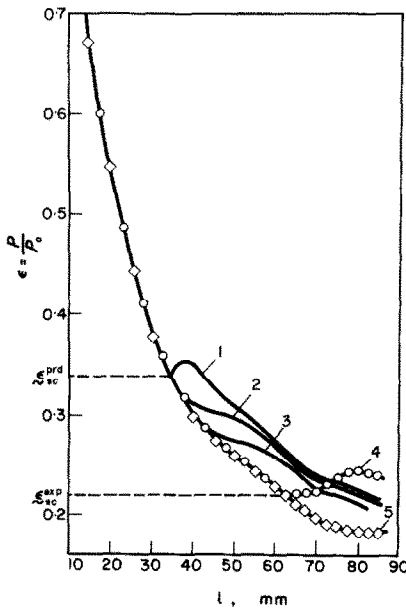


FIG. 5. Effect of condensation coefficient  $\alpha_k$  on static pressure distribution ( $P_0 = 1.49 \cdot 10^5$  N/m<sup>2</sup>;  $\beta = 1.0$ ). (1)  $T_0 = 424^\circ\text{K}$ ;  $\alpha_k = 1.0$ ; (2)  $T_0 = 424^\circ\text{K}$ ;  $\alpha_k = 0.04$ ; (3)  $T_0 = 424^\circ\text{K}$ ;  $\alpha_k = 0.0016$ ; (4)  $T_0 = 424^\circ\text{K}$ , experiment; (5)  $T_0 = 444^\circ\text{K}$ , experiment.

The main object of the analysis was to achieve the best agreement between theoretical results and experimental data with respect to all the parameters and, in particular, with respect to distribution of pressure and sizes of condensate particles. In the course of calculations the condensation coefficient  $\alpha_k$  values were varied from 1.0 up to  $10^{-3}$  and those of the coefficient  $\beta$ , from 1 up to 5.

Figure 5 presents distribution curves  $P$  predicted in an axisymmetric Laval nozzle with the help of Frenkel–Zeldovich’s equation for  $J$

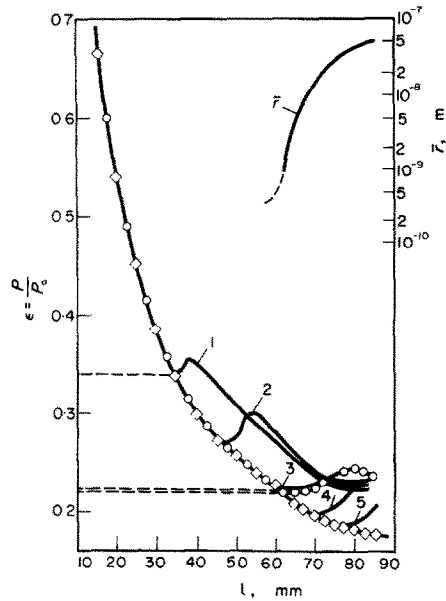


FIG. 6. Effect of factor  $\beta$  on the condensation flow behaviour ( $P_0 = 1.49 \cdot 10^5$  N/m<sup>2</sup>;  $\alpha_k = 1.0$ ). (1–6)  $T_0 = 424^\circ\text{K}$ ; (7)  $T_0 = 444^\circ\text{K}$ , experiment; (1)  $\beta = 1.0$ ; (2)  $\beta = 2.0$ ; (3)  $\beta = 3.0$ ; (4)  $\beta = 3.5$ ; (5)  $\beta = 4$ ; (6)  $T_0 = 424^\circ\text{K}$ , experiment.

( $\beta = 1$ ) and different  $\alpha_k$ . It is seen from the graphs that a considerable disagreement between the theory and experiment is found at  $\alpha_k = 1$  and  $\beta = 1$ : actually spontaneous condensation proceeds at considerably larger Mach numbers compared to the predicted ones ( $M_{kexp} = 2.05$ ;  $M_{kprd} = 1.373$ ). Variation of  $\alpha_k$  alone does not

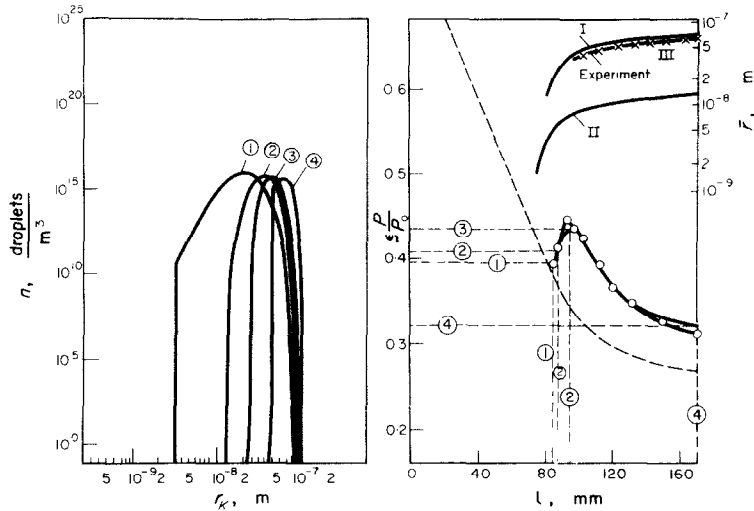


FIG. 7. Plot of pressure functions of droplet size distribution and mean droplet size along the nozzle. Curve I, predicted  $r_k$  at  $\beta = 3.0$ ; and  $\alpha_k = 1.0$ ; Curve II, predicted  $r_k$  at  $\beta = 1.0$  and  $\alpha_k = 0.04$ ;  $\alpha_T = 0.04$ ; Curve III  $r_{k/exp} = r(l)$ .

lead to the desired result. In this case pressure distribution in the condensation zone is sharply distorted in comparison with the real one, pressure peak is flattened though condensation onset still occurs at Mach numbers considerably less than  $M_{kexp}$ . Introduction of coefficient  $\beta > 1.0$  into the exponent results in displacement of the spontaneous condensation zone down the flow (Fig. 6) at  $\alpha_k = \text{const}$ . In the case under consideration good agreement of the experimental and predicted pressure distributions was obtained at  $\alpha_k = 1.0$  and  $\beta = 3$ . It should be noted that under certain conditions satisfactory agreement between predicted and experimental distributions of  $P$  may be achieved, for example, by simultaneous variation of the condensation coefficient  $\alpha_k$  and that of thermal accommodation  $\alpha_T$  [8, 9]. However, in this case a great divergence between the theoretical and experimental size distributions is usually found. Figure 7 gives values predicted by the two methods:

- (1) At  $\alpha_k = 1.0$  and  $\beta = 3$ .
- (2) Variation of  $\alpha_k$  and  $\alpha_T$ .

In both cases the predicted pressure distribution curves coincide with the experimental ones;

however, in the second case an average size of particles determined from the size distribution curve is approximately five times less than experimental  $r_k$ . At the same time agreement between particle sizes measured by the dissipation method (curve III) with those predicted by the first method at  $\alpha_k = 1.0$  and  $\beta = 3.0$  (curve I) may be considered satisfactory. The same figure gives size distribution curves for different cross-sections of a nozzle at  $\alpha_k = 1.0$  and  $\beta = 3$ .

Predictions of a condensing vapour flow performed at relatively small initial pressures  $P_0$  for different cases have also given satisfactory agreement with experimental results both on pressure distribution and on dispersion of a condensed phase. Similar predictions have also been performed at elevated pressures with  $P_0$  ranged from  $2.5 \cdot 10^5 \text{ N/m}^2$  up to  $32 \cdot 10^5 \text{ N/m}^2$ . Figure 8 exemplifies predicted curves  $\varepsilon = P/P_0 = \varepsilon(l)$  for different  $\beta$  at  $P_0 = 6.83 \cdot 10^5 \text{ N/m}^2$  and  $T_0 = 438^\circ\text{K}$ . Here it is also presented the experimental curve  $\varepsilon = \varepsilon(l)$ . As it is seen, agreement with the experiment is found at  $\alpha_k = 1.0$  and  $\beta = 3.38$ . Comparison of predictions with the experiment shows that as  $P_0$  increases,  $\beta$  should also increase, other conditions being



equal (Fig. 9). Satisfactory agreement for particle dimensions was obtained for all cases. Alongside with the experimental curve  $r_k = r(P_0)$ , Fig. 4 gives two theoretical curves, curve 1 predicted by Frenkel-Zeldovich's equation for  $\beta = 1$  [10]; curve 2 plotted by using  $\beta$ -var. Both cases gave good agreement with the experiment on pressure

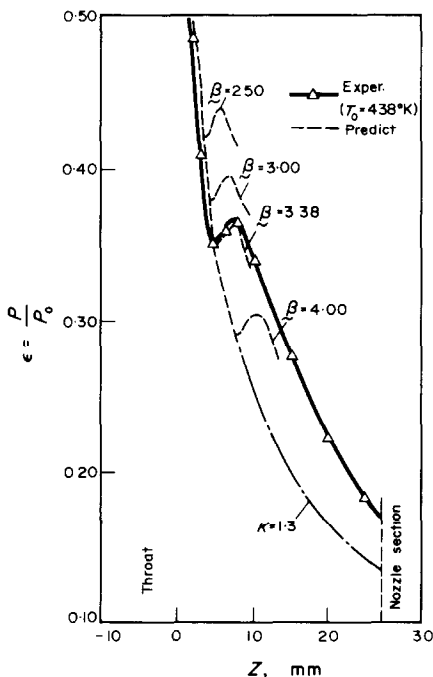


FIG. 8. Pressure distribution in an axisymmetric nozzle for  $P_0 = 6.83 \cdot 10^5 \text{ N/m}^2$ ;  $T_0 = 438^\circ \text{K}$ .

distribution. As it is seen from the graph (Fig. 4) in all cases an average dimension of particles determined in accordance with [10] is considerably less (approximately by one order) compared to experimental ones, and their concentration per mixture mass unit is respectively by two or three orders larger. At the same time introduction of the correction factor  $\beta$  gives satisfactory agreement with experimental data on dispersion in a wide range of initial parameters of saturated vapour at the nozzle inlet.

The physical significance of the factor  $\beta$  may be explained by considering the properties of

nuclei acting as condensation sites. At large subcoolings the nucleus sizes are small and comprise a small amount of molecules. For example, in steam at  $\Delta T = 45^\circ \text{K}$  and pressure  $10^5 \text{ N/m}^2$  the nucleus size is  $r_* \approx 4.1 \cdot 10^{-10} \text{ m}$ . If molecules are considered to be packed into a sphere, then in this case a nucleus contains no more than twelve molecules. It is obvious that the properties of such a cluster should differ from those of a liquid droplet containing a great amount of molecules (at very great  $r$ ).

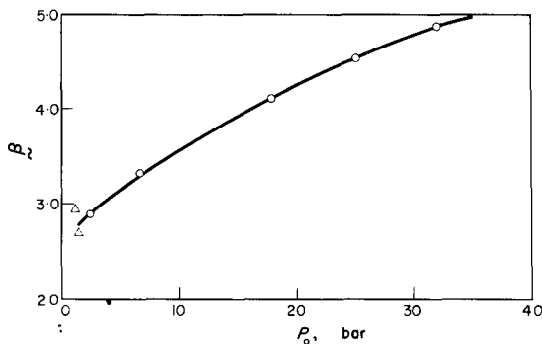


FIG. 9. Plot of  $\beta = \beta(P_0)$ .

It may be assumed that physical properties of such a cluster place it at some intermediate state between vapour and liquid phases. In this case its density as well as difference of thermodynamic potentials  $\Delta\mu$  should be less than liquid density  $\rho_k$  and potential difference found by equation (11). On the other hand, according to [3], it may be assumed that in this case the actual surface tension coefficient is somewhat less. As follows from the comparison of the theory with the experiment, the difference between the nucleus properties and those of saturated liquid obviously has a greater effect on nucleation work than a change in the surface tension coefficient. In this case  $\beta$  should exceed a unity.

In sections 1 and 2 it has been shown that the character of a pressure distribution in expanding condensing gas is mainly determined by two

effects: geometric effect and that of phase conversions. Figure 10 gives predicted curves of these effects over the nozzle for an axisymmetric nozzle (curves  $\varepsilon_{\text{exp}} = \varepsilon(l)$  for this nozzle are given in Fig. 2). It is seen that at small  $P_0$  of very intensive condensation zone the effect of phase conversions prevails over geometric effects (curves 1, 2 in Fig. 10) that leads to a considerable pressure peak in this zone (curves 1, 2, Fig.

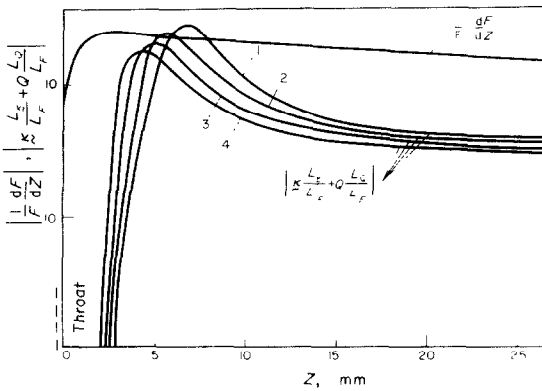


FIG. 10. Plot of phase conversion rate for increasing  $P_0$ , at  $T_0 - T \approx 4^\circ$ . (1)  $P_0 = 2.5 \cdot 10^5 \text{ N/m}^2$ ; (2)  $P_0 = 6.83 \cdot 10^5 \text{ N/m}^2$ ; (3)  $P_0 = 18 \cdot 10^5 \text{ N/m}^2$ ; (4)  $P_0 = 32 \cdot 10^5 \text{ N/m}^2$ .

2). With an increase in  $P_0$  the difference of these effects in the spontaneous condensation zone decreases; in the case under consideration at  $P_0 > (12, 13) \cdot 10^5 \text{ N/m}^2$  the geometric effect prevails over that of heat and mass transfer (curves 3, 4, Fig. 10). This leads to degeneration of pressure peak and gives rise to a favourable pressure gradient in the spontaneous condensation zone. It should be remembered that the same case is also observed at  $P_0 = \text{const}$  when a longitudinal pressure gradient (or expansion rate  $\dot{P}$ ) increases. In this case, together with deformation of the curve  $\varepsilon = \varepsilon(l)$  behind the condensation wave the degree of non-equilibrium or subcooling of the flow increases. At large  $\dot{P} \geq 10^5 \text{ I/s}$  (in case of large expansion angles, etc.) the situation is possible when behind the first zone of condensation wave a vapour

subcooling may again achieve considerable values in spite of a great number of small droplets arising in the flow at further expansion of two-phase medium. Under certain conditions this may again result in a new condensation wave.

## CONCLUSIONS

1. The theoretical and experimental investigations show that expansion of saturated and moist vapour in confusor channels are essentially non-equilibrium.

2. The comparison of the theory and experiment has shown that calculations of the nucleation rate require corrections for the work of formation of a stable nucleus of a condensed phase. This may be achieved by the correction factor  $\beta > 1$  introduced into the exponent.

3. The factor  $\beta$  increases with the initial pressure, in the range  $10^5 \text{ N/m}^2 \leq P_0 \leq 32 \cdot 10^5 \text{ N/m}^2$  it is between 2.5 and 5. The relation  $\beta = \beta(P_0)$  gives good agreement of the predicted and experimental pressure distributions and dispersity over the whole range of  $P_0$  and  $\dot{P}$  investigated of a moist vapour.

4. Other things being equal, increase of the initial pressure results in smaller maximum subcooling and flattened pressure peak in a spontaneous condensation zone. In this case a mean size of condensate particles increases. As  $P_0$  changes from  $10^5 \text{ N/m}^2$  to  $32 \cdot 10^5 \text{ N/m}^2$ , an average radius of droplets behind the condensation wave increases from  $r_k \approx 3 \cdot 10^{-8}$  up to  $r_k \approx 1.5 \text{--} 2 \cdot 10^{-7} \text{ m}$ .

5. At great  $\dot{P} > 10^5 \text{ I/s}$  phase conversions behind the first zone of spontaneous condensation may be "frozen" and a new condensation wave may appear.

6. The method proposed may be used for prediction of non-equilibrium accelerating flows with condensation in different channels.

## REFERENCES

1. K. OSWATITSCH, *Z. Angew. Math. Mech.* **22**, 1 (1942).
2. M. E. DEICH and G. A. FILIPPOV, *Two-Phase Gas Dynamics*. Izd. Energiya, Moscow (1968).

3. H. STIEVER, A condensation phenomenon in high-velocity flows, in *Fundamentals of Gas Dynamics*, edited by W. EMMONS. Princeton University Press, New Jersey (1958).
4. A. G. SUTUGIN, Spontaneous vapour condensation and aerosol formation, *Usp. Khim.* **38**, vyp. I (1969).
5. V. G. LEVICH, *Introduction to Statistical Physics*. Gostekhizdat, Moscow (1954).
6. M. E. DEICH, G. A. SALTANOV, A. V. KURSHAKOV and I. A. YATCHENI, A study of phase transition kinetics in shock waves in moist vapour flows, *Teploenergetika*, No. 4 (1971).
7. M. E. DEICH, A. V. KURSHAKOV, G. A. SALTANOV and I. A. YATCHENI, A study of two-phase flow structure behind condensation wave in supersonic nozzles, *Izv. AN SSR, Energetika i Transport*, No. 2 (1969).
8. R. PUZYREWSKI, Kondensac ja pary wodney w dyszy de Lavala, *Inst. Maszyn przeplywowych*, PAN, Warszawa (1967).
9. V. P. BAKHANOV and M. V. BUIKOV, Kinetics of quasi-stationary homogeneous steam condensation in a supersonic nozzle, in *Physics of Aerodispersed Systems*. Izd. KGU, vyp. 2 (1970).
10. G. GYARMATHY, *Gründlagen einer Theorie der Nassdampfturbine*. Zurich (1962).

#### GENERATION ET CROISSANCE D'UNE PHASE CONDENSEE DANS DES ECOULEMENTS A GRANDE VITESSE

**Résumé**—On considère les résultats théoriques et expérimentaux de la condensation spontanée de vapeur dans des tuyères supersoniques. Les recherches expérimentales ont été conduites dans le domaine de pressions initiales de  $10^5$  N/m<sup>2</sup> à  $32 \cdot 10^5$  N/m<sup>2</sup> à l'aide de méthodes optiques et thermopneumométriques. Les mesures concernent le début de la condensation, la forme de la zone d'intense conversion de phase, les dimensions des particules mesurées par un laser Ne-He selon la méthode d'indicatrice dissymétrique. Des calculs ont également été faits. On montre que l'introduction du coefficient  $\beta > 1$  qui est pour le travail de nucléation une correction de l'exposant de la vitesse de nucléation, établit un bon accord entre les valeurs estimées et expérimentales à la fois pour la distribution de pression et les dimensions des particules. La relation entre  $\beta$  et  $P_0$  dans le domaine de pression considéré est obtenue par comparaison entre les résultats expérimentaux et théoriques.

#### ERZEUGUNG UND WACHSTUM DER KONDENSIERENDEN PHASE IN STRÖMUNGEN HOHER GESCHWINDIGKEIT

**Zusammenfassung**—Die theoretischen und experimentellen Ergebnisse bei der spontanen Dampf-kondensation in Überschalldüsen werden dargelegt. Im Ruhedruckbereich von  $10^5$  N/m<sup>2</sup> bis  $32 \cdot 10^5$  N/m<sup>2</sup> wurden experimentelle Untersuchungen mit Hilfe optischer und thermopneumatischer Methoden durchgeführt. Die Daten wurden bei Kondensationsbeginn aufgezeichnet in einer Zone intensiver Phasenumwandlung. Die Teilchengrößen wurden nach der Methode der Indicatrix-Asymmetrie mit Hilfe eines He-Ne-Lasers bestimmt. Es wird gezeigt, dass durch die Einführung des Koeffizienten  $\beta > 1,0$ , der eine Korrektur für die Keimbildungsarbeit darstellt und als Exponent in die Keimbildungsrate eingeht, gute Übereinstimmung zwischen den berechneten und experimentellen Werten erzielt wird, sowohl für die Druckverteilung als auch für die Teilchengröße. Die Beziehung zwischen  $\beta$  und  $P_0$  im untersuchten Druckgebiet wird erreicht durch Vergleich der experimentellen und berechneten Werte.

#### ЗАРОЖДЕНИЕ И РОСТ КОНДЕНСИРОВАННОЙ ФАЗЫ В ВЫСОКОСКОРОСТНЫХ ПОТОКАХ

**Аннотация**—Рассмотрены результаты теоретических и экспериментальных исследований спонтанной конденсации водяного пара в сверхзвуковых соплах. Экспериментальные исследования проводились в диапазоне начальных давлений от  $10^5$  н/м<sup>2</sup> до  $32 \times 10^5$  н/м<sup>2</sup> оптическими и термопневмометрическими методами. Получены данные по определению начала конденсации, формы зоны интенсивных фазовых превращений, размерам частиц, измеряемым методом асимметрии индикатрисы с помощью Ne-He лазера. Проведены расчеты таких течений. Показано, что введением в экспоненту скорости ядрообразования коэффициента  $\beta > 1,0$ , корректирующего работу образования зародышей, удается получить хорошее совпадение теории с опытом как по распределению давления, так и по размеру частиц. На основании сравнения экспериментальных и расчетных данных получена зависимость  $\beta$  от  $P_0$  в исследуемом диапазоне давлений.